

# FIELD EMISSION IN SRF ACCELERATORS: INSTRUMENTED MEASUREMENTS FOR ITS UNDERSTANDING AND MITIGATION\*

R. L. Geng<sup>†</sup>, A. Freyberger, R. Legg, R. Suleiman, JLAB, Newport News, VA, USA  
A. S. Fisher, SLAC, Menlo Park, CA, USA

## Abstract

Several new accelerator projects are adopting superconducting RF (SRF) technology. When accelerating SRF cavities maintain high RF gradients, field emission, the emission of electrons from cavity walls, can occur and may impact operational cavity gradient, radiological environment via activated components, and reliability. In this talk, we will discuss instrumented measurements of field emission from the two 1.1 GeV superconducting continuous wave (CW) linacs in CEBAF. The goal is to improve the understanding of field emission sources originating from cryomodule production, installation and operation. Such basic knowledge is needed in guiding field emission control, mitigation, and reduction toward high gradient and reliable operation of superconducting accelerators.

## INTRODUCTION

Field emission (FE) is a well-known phenomenon in both normal conducting and superconducting RF cavities. Its impact to SRF cavities is far more profound owing to the fact that the surface power dissipation in SRF cavities is smaller by many orders of magnitude as compared to their normal-conducting counterparts. Therefore, there is significant interest in its understanding and control for SRF accelerator design, construction and operation.

Despite the continued progress in understanding and control of FE over decades, the challenge remains as the specification of operation gradients has been on the rise too. By using today's state-of-the-art cavity surface processing and assembly techniques, FE is controlled satisfactorily in qualified individual cavities. This has been demonstrated in SRF accelerator projects requiring large numbers of multi-cell cavities prepared and assembled in laboratories as well as in industry [1,2]. However, preserving the cavity performance from qualification testing of individual cavities to SRF cryomodule operation with beam remains an issue of interest. One cause for cavity performance loss is the degradation of FE onset and this has provoked lots of recent discussions [3].

It is generally believed that the current understanding of the basic physics of FE in SRF cavities is adequate [4-6]. The challenge lies largely in the engineering aspects of controlling *field emitter input or activation* over the course of constructing, shipping, commissioning and operating the SRF cavities at an increasingly complex level of cryomodules, segments, and linacs. In such a situation, oppor-

tunities for learning and improving are rather scarce because of limited number of large-scale SRF projects and yet a closed loop is required to allow understanding and testing. Fortunately, some recently completed SRF projects, such as CEBAF 12 GeV upgrade and E-XFEL, have provided new opportunities. Looking forward, several new accelerator projects are adopting SRF technology, such as ESS, FRIB, LCLS-II etc., one may anticipate a continued progress in our understanding and mitigation of FE in SRF accelerators. In this paper, we present our instrumented measurements of FE from the two 1.1 GeV superconducting CW linacs in CEBAF. This work is based on and an extension of the previous work in our effort of FE understanding for its ultimate control, in particular for large scale CW SRF accelerators [7].

## FE THEORETICAL AND PRACTICAL

### FE Theory

The original theory of FE was developed by Fowler and Nordheim [8]. It describes electron emission in electric fields at the interface of a metal and a vacuum based on the quantum mechanical tunnelling process. The potential barrier at the interface prevents electrons in the metal from escaping. The work function  $\phi$ , a material dependent property, is the measure of this barrier.  $\phi = 3-5$  eV for most metals. When no external electric field is applied to the metal surface, electrons in the metal are confined as they are at the Fermi energy level which is below the vacuum energy level by an amount of the work function and the thickness of the potential barrier is infinite. An external electric field applied to the metal surface  $E_s$  deforms the original rectangular potential barrier of infinite thickness into a triangular barrier of finite thickness, thus permitting electron tunnelling with finite probability. The salient result of the FN theory is that the FE current density  $j_{FN}$  rises exponentially with an increasing electric field:  $j_{FN} = (A E_s^2 / \phi) \exp(-B \phi^{3/2} / E_s)$ , where A and B are constants.

The agreement between experimental results and the FN theory is quite satisfactory provided the surface electric field  $E_s$  is replaced by  $\beta_{FN} E_s$ , where  $\beta_{FN}$  is the field enhancement factor [9,10].  $E_s$  and  $\beta_{FN}$  are typically in the range of 10-100 MV/m and 50-1000, respectively in SRF cavities. Besides  $\beta_{FN}$ , the effective emitting area  $A_e$  is a parameter useful for fitting the total FE current  $I_{FN} = j_{FN} A_e$  against the FN law.

### FE in SRF Cavities

The estimated time for an electron to tunnel through the potential barrier is on the order of fs, orders of magnitude smaller than the ns RF period for typical SRF applications

\* Authored by Jefferson Science Associates, LLC under U.S. DOE Contract No. DE-AC05-06OR23177. The U.S. Government retains a non-exclusive, paid-up, irrevocable, world-wide license to publish or reproduce this manuscript for U.S. Government purposes.

<sup>†</sup> geng@jlab.org

[11]. Therefore, the FE process in SRF cavities can be regarded as instantaneous. It then follows that the RF FE current  $I_{FN}(t)$  at the emitting site is periodic as the emission is permitted only when the instantaneous local field is pointed toward the surface. Consequently, electrons are field emitted in pulsed mode with a repetition rate identical to the frequency of the RF field in the cavity.

Figure 1 shows two hypothetical FE scenarios in a 7-cell 1.5 GHz CEBAF 12 GeV upgrade SRF cavity with an acceleration gradient  $E_a=15$  MV/m. The upper graph depicts trajectories of electrons emitted from a site close to the iris between the 3<sup>rd</sup> & 4<sup>th</sup> cavity cell. Due to the finite spread in the emission phase, electrons emitted from the same point trace out a family of trajectories. Electrons gain energy from the EM field. Some get lost as they hit cavity walls but some survive and reach the borders of the simulation (vertical line at both ends). Those striking the wall give up their gained energy predominantly in the form of heat. Bremsstrahlung X-rays are created as well. Those surviving from wall hitting then export themselves into the neighbouring cavity in case of a string of cavities being laid in tandem (such as in a cryomodule). The lower graph depicts trajectories with the emitting site slightly moved away from the site in the upper graph.

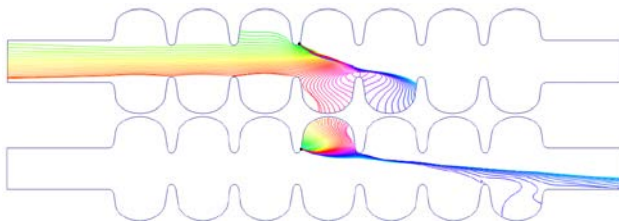


Figure 1: Family of trajectories for electrons emitted from two slightly separated emitting sites in a 7-cell 1.5 GHz CEBAF 12 GeV upgrade SRF cavity at  $E_a = 15$  MV/m.

It is noteworthy that as illustrated in Fig. 1 that, depending on the exact location of the emitting site, FE electrons can export themselves into either the upstream cavity or downstream cavity. The exported electrons can gain significant energy (scales as  $E_a L$ , where  $L$  is the separation between the emitting site and the export plane) arising from phase synchronization. In principle, electrons emitted from the end cells can gain the full RF voltage. When the emitting site is further moved away from the iris, most FE electrons will get lost in the mid-cell.

It should be mentioned that, on a theoretical ground, due to the existence of an energy gap, a small difference in the FE current is predicted when a metal makes a transition from its superconducting state to normal conducting state. However, no difference of practical significance has been experimentally measured [12]. In addition, as will be shown later, FE in SRF cavities is mostly originated from foreign particulates adhering to niobium surfaces. Therefore, superconductivity does not impose any special concern in view of FE. However, SRF cavities must work at cryogenic temperatures. The cold cavity surface cryopumps residual gas molecules. These adsorbed species do have strong influence in FE behaviours under some circumstances. This point will be touched upon later.

## Field Emitters

As a result of past studies, the present view is such that FE in SRF cavities is originated from *localized sites* on the inner cavity surface. The predominant source emitters are microscopic particulates adhering to the inner cavity surface, chemical residuals, and geometrical flaws [13].

Some of the particulate field emitters are introduced by the necessary chemical surface processing which transforms the raw inner surface of an as-built cavity into a high quality working surface able to hold high surface electromagnetic fields. Although the post chemistry ultrasonic cleaning and high pressure water rising remove most particulates and flush them out of the cavity, some may still remain due to either a stronger particle-surface adherence force or varying distribution of the dislodging force delivered to the location where a particle resides.

Other particulate field emitters are introduced through the cavity opening ports onto the cavity surface, at a time beyond the completion of final cleaning, from external sources. Examples are airborne particulates, debris generated from handling, tooling, flange jointing, gasket crashing, gate valve actuating, ion pump starting and operating etc. To minimize this *field emitter input*, SRF cavities are assembled in large-sized high-quality Class 10 (ISO 4) cleanliness clean rooms into cavity strings; critical assembly steps are done with the opening port facing down; cavity strings are evacuated slowly etc. These equipment and procedures reduce particulate input by lowering either the number of external source particles or the chance of external particulates being transported into the cavity. Particulate transportation can be enabled by gravitational pull or mechanical energization (shocking impact at cavity bodies, turbulent flow in vacuum ducts etc.).

For illustration, Fig. 2 shows a typical stainless steel particulate that was collected from a CEBAF-type 5-cell niobium SRF cavity after service for beam operation [14].

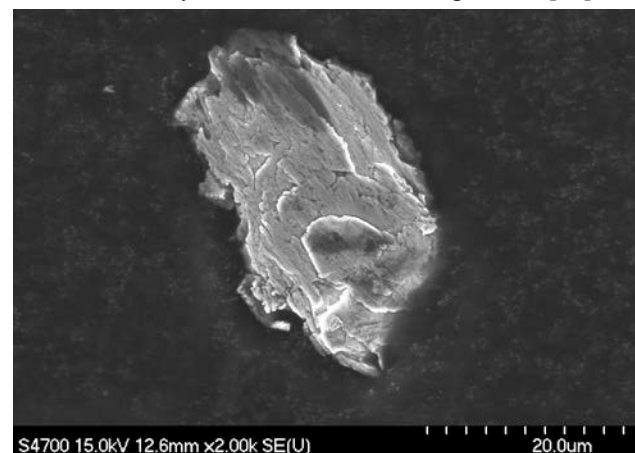


Figure 2: A typical stainless-steel particulate collected from a CEBAF-type 5-cell niobium SRF cavity.

Geometrical flaw field emitters, such as protrusions and scratches, are still encountered but their occurrence is significantly lower than particulate field emitters in modern cavities. This may be a result of broadly adopted elec-

tropolishing surface processing which gives a smooth surface and is particularly effective in reducing sharp protruding tips in the iris regions of SRF cavities. In addition, FE caused by a geometrical flaw tends to be stable and insensitive to additional cleaning such as repeated high pressure water rinse [15]. As a result, cavities strongly affected by this kind of field emitters are likely rejected from further string assembly and will not make it to the accelerator (of course such cavities can be repaired and may be used afterwards still). In the context of this talk, we will not discuss this kind of field emitters any further.

### FE Instrumentation

In the past, several kinds of instrumentation have been successfully used for studying FE in SRF cavities in laboratory testing studies [16].

- **Temperature monitoring/mapping:** temperature sensors (carbon resistors) attached to the outer surface of a cavity immersed in liquid helium bath detect heat deposited by FE electrons [17-19].
- **Electron detecting:** Metal probes inserted into the cavity space or RF antenna probes, positively biased, collect FE electrons [17,18,20].
- **X-ray monitoring/mapping:** radiation sensors or detectors (photodiodes, ionization chambers, NaI scintillators) placed in liquid helium bath near a cavity or in the air outside Dewar detect intensities and energy spectrums of Bremsstrahlung X-rays induced by FE [4,20,21]. Arrays of detectors (rotating or fixed) near cavity walls detect simultaneously to reconstruct X-ray intensity 3D map [18,21,22]. Detectors traveling on a linear rail trace out X-ray intensity 1D distribution [23].
- **X-ray photography:** “pin hole camera” placed outside of testing Dewars image the X-ray intensity 2D distribution on a film [24,25].
- **Optical imaging:** cameras with line-of-sight view of the cavity inner space image luminous spots arising from light emission at FE emitting site or luminous objects in the vacuum space [26,27].

These FE instrumentation played a key role in understanding the basics of FE in SRF cavities, such as establishing the exponential nature of FE consistent with the FN law, establishing the point-like nature of field emitters, identifying the locations of field emitter sites when the data are analysed in conjunction with the computer-aided calculations of electron trajectories.

### Degradation of FE Onset from Vertical Test to Cryomodule Placement in Tunnel

It is common practice across SRF testing facilities to monitor FE by detecting Bremsstrahlung X-rays with detectors placed outside of Dewars for vertical testing of individual cavities or outside of cryomodules for cryomodule testing. A useful figure of merit is the FE onset, the accelerating gradient at which the first FE induced X-ray being detected. Degradation in the FE onset from vertical qualification testing of a cavity to its verification testing in a cryomodule has been observed. Further degradation may

be observed as well at the point of cryomodule commissioning test in the accelerator tunnel. This issue of FE onset degradation has attracted broad international interest for its understanding and mitigation [3]. It is commonly believed this degradation is caused by *particulate input* onto the cavity surface arising from handling and assembly of components beyond the final cavity acceptance test, therefore such degradation might be preventable, or at least can be reduced, by executing strict handling and assembly procedures.

It has been recognized that improved FE instrumentation is needed for understanding the FE onset degradation from cavity vertical testing to cryomodule placement in accelerator tunnels. Presently there are variations in X-ray detector types, cavity-detector distances, materials between the cavity and the detector etc. across SRF facilities, and even within the same facility. This situation leaves ambiguity in quantifying the FE onset degradation or for comparing the degradation among multiple facilities.

An effort has been made recently at JLab by placing a permanent photodiode (Hamamatsu S12230-1 PIN diode) next to each cavity in a cryomodule [28]. In total, 16 diodes were placed in that cryomodule, one each at each end of the eight 7-cell cavities contained (see Fig. 3). The vertical testing of each cavity was instrumented with the same kind of photodiode maintaining the same spatial relationship with respect to the cavity. This effort was aimed to improve the certainty in judging the FE onset degradation from cavity vertical testing to verification testing in a cryomodule at various checking points. These permanent photodiodes might be useful for FE instrumentation during routine beam operations. A test is presently being conducted by instrumenting LCLS-II cryomodules with an optical fiber based X-ray detection system. By maintaining a fixed spatial arrangement with respect to the cavity string contained in a cryomodule, this system leads to a site-independent measurement of FE, permitting comparisons between testing facilities at JLab and FNAL. The optical fiber is expected to be used in SLAC tunnel for beam loss detection and FE detection as well.

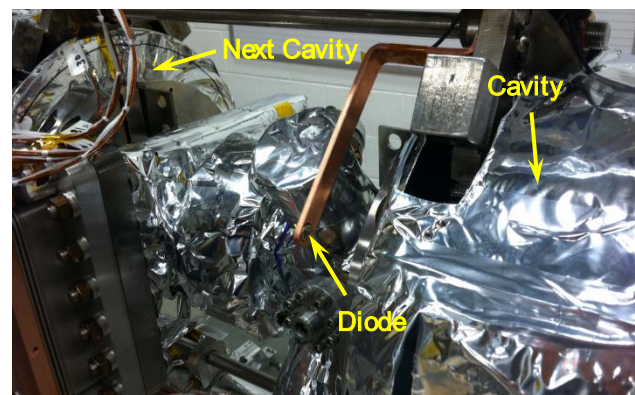


Figure 3: A photodiode placed next to a cavity permanently for FE instrumentation in a CEBAF-type cryomodule.

## FE IN SRF ACCELERATORS

FE in SRF accelerators may have impacts to the accelerator energy reach, reliability and maintainability. We will

limit the discussion on large scale CW SRF linacs with a focus on the 12 GeV CEBAF. However, many aspects to be discussed may be relevant to other kind of SRF systems such as pulsed SRF linacs, in particular those linacs adopting the CEBAF-type cryomodule topology (SNS, ESS).

Presently, CEBAF consists of two 1.1 GeV SRF linacs [29]. Each linac consists of 20 original CEBAF cryomodules (each provides a nominal acceleration voltage of 20 or 50 MV, dubbed as C20 or C50) plus 5 upgrade cryomodules (nominal voltage 100 MV, C100). In total, 418 multi-cell cavities are presently installed in CEBAF.

### FE Impact to CEBAF Operation

Several aspects must be considered to properly understand the implication and impact of FE to CEBAF:

- FE electrons may affect ceramic windows in RF input couplers causing fast trips as was understood for C20 cryomodules.
- Field emitted electrons may be captured and exported out of the source cavity. These electrons may propagate into other cryomodules and gain increasingly larger energies, resulting in steep radiation damage.
- Cold cavities are open to the vacuum spaces of warm beamline components, resulting in a continued *gas input* into the cavity. The frozen gases may activate new field emitters or enhance FE of existing field emitters arising from the resonant tunnelling effect [4,30,31]. Particulates may be generated from movement of beamline components such as cycling of gate valves. This may lead to *particulate input* into cavities directly or enabled by other mechanism [7].
- The accelerator must be operated at required beam energies and simultaneously with required beam reliability. Pushing the accelerating gradient for higher beam energies may decrease the system reliability when FE is present because of the exponential field dependence of FE.

To improve our understanding of these aspects, several tests have been carried out at CEBAF since January 2016 with instrumented measurements of FE at various zones with various types of radiation detectors.

### Propagation of Field Emitted Electrons

Several tests were performed in different zones to study propagation of field emitted electrons. Tests done in the injector zones 0L03 (C20 cryomodule) and 0L04 (C100 cryomodule) were instrumented with an SNS-type fast beam loss monitor (plastic scintillator + PMT by Bridgeport, model R2D-FBLM-138) attached to the downstream endplate of cryomodule in zone 0L04 (see Fig. 4). This detector was operated in the pulse counting mode with an exiting DAQ system. The X-ray count rate was less than 10 Hz with zone 0L04 on and operated at nominal gradients while leaving zone 0L03 off, indicating no detectable FE from 0L04. The count rate went to  $10^4$  Hz by turning zone 0L03 on at nominal gradients while leaving zone 0L04 off, indicating FE sources being present in 0L03. This count rate

went up to  $10^6$  Hz when zone 0L04 was turned on while maintaining 0L03 on. This experiment shows that electrons field emitted from zone 0L03 were propagated into zone 0L04.

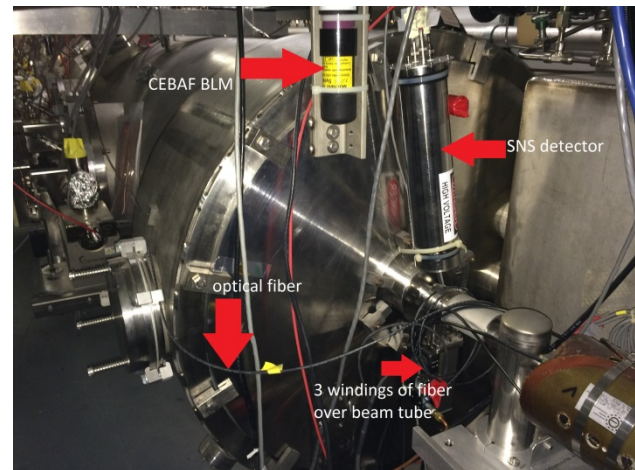


Figure 4: FE testing in CEBAF injector zones 0L03 & 0L04 with a SNS-type detector attached to the downstream endplate of the cryomodule in zone 0L04.

A set of tests was performed in zones 1L25 and 1L26 (both C100 cryomodules) of the North Linac with four high dose rate ion chambers placed adjacent to cryomodules [32]. It was found that FE electrons can be accelerated up and downstream in the C100s between cryomodules. Radiation levels produced by the transmitted electrons go as the ratio of their energy.

An interesting observation was made on November 11, 2016 as shown in Fig. 5. Two ion chambers (one each upstream 1L25 & 1L26) both reacted to gradient changes in zone 1L11, 12 & 13. Gradient scanning at zone 1L22 had no impact. All other cryomodules in North Linac were at nominal gradients. This observation seems to indicate that FE electrons are propagated over a remarkable long distance (> 100 m) passing multiple (15) cryomodules.

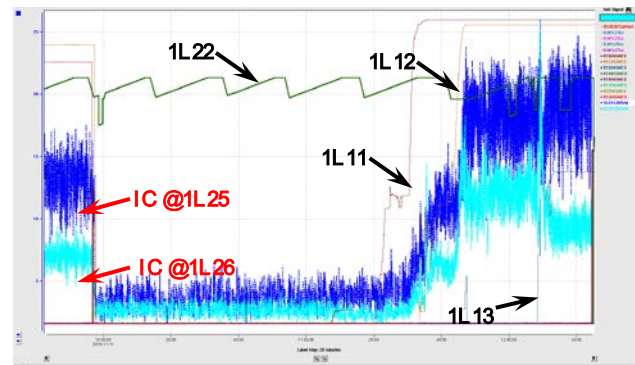


Figure 5: Ion chambers (IC) at zone 1L25 & 1L26 react to sum module gradients at zone 1L11, 12 & 13.

Now that it is known that field emitted electrons can be exported out of the source cavity in either direction and be propagated into near or even far cryomodules, we may come up with some general guide lines for FE mitigation.

- It is useful to know which cavity is a FE source cavity. Turn its gradient down.

- It is useful to preferentially place FE-free cryomodule upstream of a linac and heavy FE cryomodule downstream.
- It is useful to choose a set of inter-cavity spacing and inter-cryomodule spacing such that the backward propagation of field emitted electrons can be reduced (the forward propagation cannot be mitigated by this technique due to requirement for the main electron beam).

Due to the exponential field dependence of FE, tuning the source cavity gradient can have a major effect. For example, one FE test in zone 1L25 & 1L26 with ion chamber monitors shows that radiation levels are changed by 50% when a 3% change in gradient made.

The lost gradient due to lowering the source cavity can be restored by raising the gradient of FE-free cavities. A proof-of-principle test of this *gradient re-distribution for reducing FE radiation* was done in zone 0L03 & 0L04 as shown in Fig. 6. By scanning the individual cavities contained in 0L03 & 0L04, two FE source cavities were identified, 0L03-3 & -7. By lowering the gradient of each of them by 3 MV/m and raising the gradient of two FE-free cavities (0L03-5 & -6) by 3 MV/m, the FE induced X-ray count rate was reduced from  $6 \times 10^5$  to less than 10 Hz with the integrated acceleration voltage still preserved.

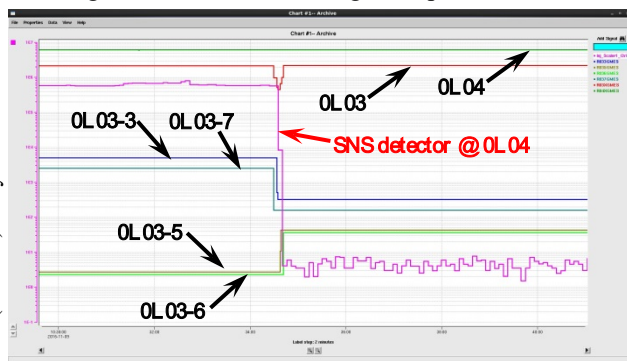


Figure 6: Reducing FE X-rays by gradient re-distribution.

### FE Turn-On Event and Possible Trigger

As described in [33], it has been found out recently that many permanent beam loss monitors (BLMs) are sensitive to FE induced radiation. A CEBAF BLM is a PMT (Burle 931B) built into a housing made of ABS plastics [34]. Its working mechanism is scintillation and Cherenkov radiation in the glass envelope of the tube. Nearly each cryomodule in CEBAF has a BLM attached to its upstream endplate. Figure 7 shows an example at zone 0L04. A pattern was found that a BLM has a preferential sensitivity to radiation induced by FE originating from cavities contained in its upstream cryomodule. As their signals are archived together with other machine data such as cavity gradients, beamline vacuum levels, a possibility arises in using their signals for long term monitoring of FE in each module in CEBAF. Aided by the ion chambers mentioned in previous section, a crude calibration was carried out permitting a rough estimation of the radiation dose rate [33].

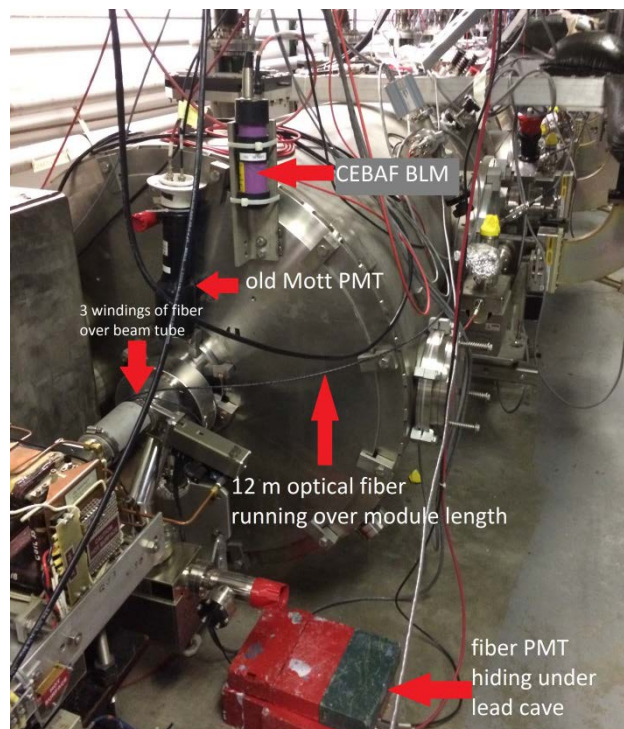


Figure 7: A CEBAF BLM (purple tube in the upper center of the photograph) attached to the upstream endplate of the cryomodule 0L04.

Here we give one example of exploiting BLMs for detecting a giant FE turn-on event. Figure 8 shows the sum gradient of cryomodule 2L26 and the signal of the sensitive BLM (in this case the BLM attached to the downstream endplate of the cryomodule at zone 2L26) for the period of December 1 – 16, 2016. The trend of the BLM signal tracks that of the sum gradient, indicating the sensitivity. This correlation was broken around 5:25 on December 13, 2016. The radiation dose rate jumped up from 1 to  $10^4$  R/h, indicating a giant FE turn-on.

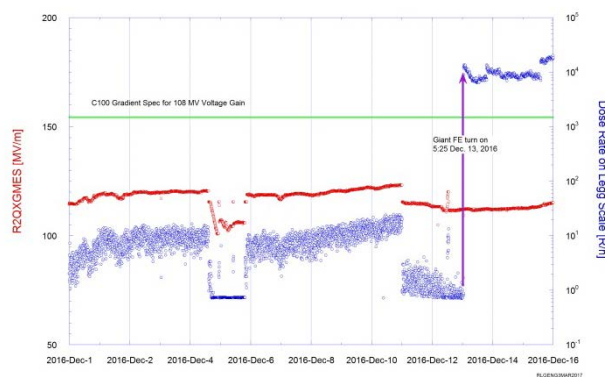


Figure 8: Jump in radiation signal (blue) of the BLM sensitive to FE originated from the cryomodule at zone 2L26, indicating a FE turn-on. The sum gradient in red.

An analysis of this event was carried out, suggesting this FE turn-on was probably triggered by frozen gases. A detailed view of the BLM raw signal for a ~ 14 minute period is shown in Fig. 9.

Content from this work may be used under the terms of the CC BY 3.0 licence (© 2018). Any distribution of this work must maintain attribution to the author(s), title of the work, publisher, and DOI.

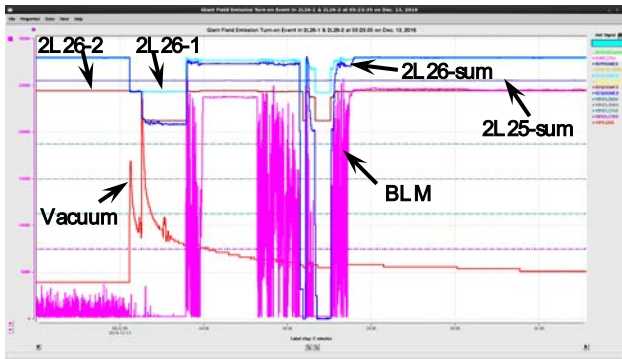


Figure 9: FE turn-on event in cryomodule at zone 2L26. FE induced radiation is reflected by the BLM signal.

The event began with the collapse of the gradient of cavity 2L26-1 at 05:22:13 (the CEBAF beam was lost at his instant) and collapse of the gradient of 2L26-2 17s later. Other cavities were stable. Each gradient collapse was accompanied with a jump in the beamline vacuum pressure (from  $2 \times 10^{-9}$  to  $4 \times 10^{-8}$ , then to  $2 \times 10^{-7}$  torr) measured by the ion pump attached to the warm beamline immediate upstream of cavity 2L26-1. When both collapsed gradients were brought back at 05:23:35, the radiation level saw a large jump. Thereafter, the gradients of cavity 2L26-1 & -2 collapsed two more times (which also triggered gradient collapse in other 2L26 cavities) and the radiation levels were quite noisy while the sum gradient was restored. Finally, at 05:27:31, both the cavity gradients and the beamline vacuum pressure restored to their pre-event levels, but the radiation level stayed at a high level. The CEBAF beam was restored shortly after. It is noted that 2L26 is the last cryomodule in South Linac and the sum gradient in the upstream cryomodule was stable over the course of the entire event. Although we cannot rule out other explanation with regard to the trigger of this FE turn-on event, the most likely one is the following: gas molecules released from cold surfaces arising from gradient collapse in cavity 2L26-1 & -2 re-condensed onto some field emitters initially field emitting mildly. The newly condensed gas molecules significantly enhanced the FE due to the resonant tunnelling effect [4,30,31].

It should be mentioned that the sudden FE turn-on event documented above is not uncommon at all as revealed by comprehensive analyses of the BLM signals for all C100 cryomodules where sensitive BLMs exist for the period from October 2014 to February 2017. Correlation between FE turn-on and beamline vacuum pressure bursts is observed in other cryomodules such as in 1L23.

In the meantime, a beneficial effect is also observable in which the BLM signal decreases slowly with time over the period of accelerator operation for physics programs, indicating gradual weakening of active field emitters. Such an effect is consistent with the ordinary “RF processing effect” of field emitters [10].

It should also be mentioned that “abrupt changes” in the slope of FN fitting for the inverse of trip interval observed in original CEBAF cavities were interpreted as changes in FE and it was speculated that adsorbed gases caused those changes [35,36].

Given what we have recently learned on the FE behaviors in C100 cavities directly measured by CEBAF BLMs since 2014, it appears that the frozen gases may indeed play some role in activating new field emitters in cavities placed in the CEBAF tunnel. A recent analysis of frozen gases condensed onto cold surfaces of C100 cavities revealed that  $H_2$  alone can accumulate up to 3 monolayers in the worst case while in most case  $H_2$  accumulates at a rate faster than expected [37].

In view of the available evidence and our current understanding of FE in CEBAF cavities enabled by FE instrumentation, one can expect FE reduction by reducing gas input into SRF cavities, in particular C100 cavities. Until a method is found for removing particulate field emitters, frozen gas removal should be aggressively pursued to check if degradation in the FE onset can be reversed. This includes not only helium processing cold cavities but also room temperature warmup of cryomodules and an improved beamline vacuum system.

### Testing Optical Fiber and Diamond Detectors

As mentioned earlier, new detectors are of interest to us. For this reason, testing of a radiation resistant optical fiber and two types of diamond detectors (Cividec B2 & B4) was carried out at CEBAF in January 2017. One each diamond detector was placed up and downstream of the cryomodule at zone 1L26 in North Linac. A 12-m long optical fiber was laid across the 8-m long cryomodule. At both ends, the fiber made three turns around the beampipe. Figure 10 shows the upstream view of the cryomodule. The optical fiber was later on further tested in the injector at zone 0L04 as can be seen in Fig. 4 & 7.

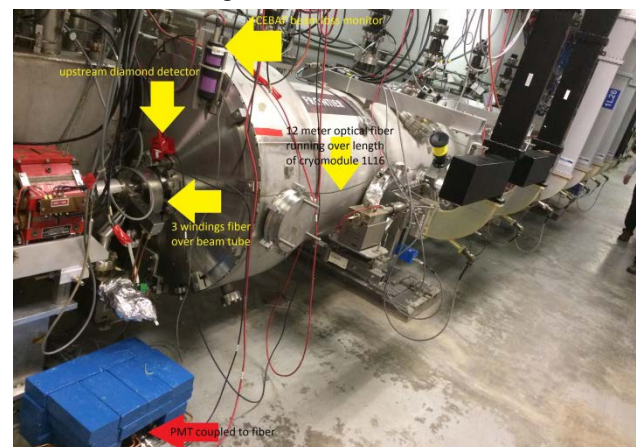


Figure 10: Upstream view of the C100 cryomodule at zone 1L26. The upstream diamond detector, optical fiber and its PMT hidden in a cave made of lead bricks are visible as well as the CEBAF BLM.

Compared to the BLMs and diamonds, the fiber was significantly more sensitive to signals from the interior cavities of cryomodule at zone 1L26, and less sensitive to crosstalk from cryomodule at zone 1L25. This is consistent with its location, draped along the full length of the tank, which should make it sensitive to all cavities, but much less sensitive to the neighbouring cryomodule.

## CONCLUSIONS

In this talk, we have discussed instrumented measurements of FE from the two 1.1 GeV superconducting CW linacs in CEBAF. Although the effort is still in its early stage, the initial results have shed new lights in our understanding of the unique aspects of FE in an operational SRF linac. Some guidelines are given for field emission reduction and mitigation. New detectors have been tested and an optical fiber emerges as a useful alternative for its sensitivity to inner cavities in a cryomodule.

Future developments are needed in testing radiation hard detectors both for X-ray intensity and energy spectrum measurements, 3D X-ray mapping or imaging for field emitter localization in conjunction with computer simulation of FE electron movement, FE monitoring with permanent detectors placed at individual cavities in cryomodules for optimizing accelerator beam operation at high energy gain and simultaneously low radiation production and low trip rate. It seems that much understanding and benefit can be gained by equipping cryomodules with FE sensors from the design phase of cryomodules. This will permit continued diagnostic of FE over the full course of cryomodule assembly, installation and operation and ultimately lead to high gradient and reliable operation of superconducting accelerators.

## ACKNOWLEDGMENT

RLG is indebted to Sasha Zhukov of ORNL for loaning a SNS beam loss monitor. He also wants to thank Tommy Michaelides for help in providing technical information of the CEBAF beam loss monitors.

## REFERENCES

- [1] A. Burrill et al., "SRF cavity performance overview for the 12 GeV upgrade," in *Proc. IPAC'12*, New Orleans, LA, USA pp.2423-2425 (2012).
- [2] D. Reschke et al., "Performance in the vertical test of the 832 nine-cell 1.3 GHz cavities for the European x-ray free electron laser," *Phys. Rev. Accel. Beams* 20, 042004(2017).
- [3] See talks presented at the 2017 TESLA Technology Collaboration (TTC), Working Group 2: Performance Degradation, Cure, Beamline Quality. <https://indico.fnal.gov/conferenceTimeTable.py?confid=12662#20170221>
- [4] H. A. Schwettman, J. P. Turneure, R. F. Waites, M. Jimenez, "Radiofrequency field-emission studies. II" initial experimental results," *Appl. Phys.* 45 (1974) 914.
- [5] J. Knobloch, H. Padamsee, Part. Accel. "The science and technology of superconducting cavities for accelerators," (1996) 53.
- [6] A. Navitski et al., "Field emitter activation on cleaned crystalline niobium surfaces relevant for superconducting rf technology," *Phys. Rev. Spec. Topic - Accel. and Beams*, vol. 16 p. 112001, 2013.
- [7] R. L. Geng, "Status of the Short-pulse x-ray project at the advance photon source," *Proc. IPAC'16* pp. 3198-3201 (2016).
- [8] R. H. Fowler and L. Nordheim, "Electron Emission in Intense Electric Fields," *Proc. R. Soc. Lond.* A119 (1928) 173.
- [9] R. J. Noer, *Appl. Phys.* A 28 (1982)1.

- [10] See Ch. 12, H. Padamsee, J. Knobloch, T. Hays, "RF superconductivity for accelerators," John Wiley & Sons, (1998).
- [11] B. Bonin, *Proc. CERN Accelerator School. CERN 96-03* (1996)221.
- [12] R. Klein and L.B. Leder, "Field emission from niobium in the normal and superconducting states," *Phys. Rev.*, vol. 124, p. 1050, 1961.
- [13] D. Reschke, "Cleanliness Techniques," *Proc. SRF2005* pp.71-77 (2005).
- [14] R. L. Geng et al., "Nature and implication of found actual particulates on the inner surface of cavities in a full-scale cryomodule previously operated with beam" *Proc. SRF2015*, MOPB035, pp.164-168 (2015).
- [15] R. L. Geng, T. Goodman, Jefferson Lab internal report, JLAB-TN-11-006 (2011).
- [16] P. Kneisel, Jefferson Lab internal report, JLAB-TN-11-006 (2011).
- [17] K. Yoshida, M. Yoshioka, and J. Halbritter, "Measurements of superconducting niobium cavities at 700 MHz," *IEEE Trans. Nucl. Sci.*, vol. NS-26, p. 4114, 1979.
- [18] Ph. Bernard et al., "Experiments with the CERN superconducting 500 MHz cavity," *Nucl. Instr. Meth.*, vol. 190, p. 257, 1981.
- [19] J. Knobloch, "Metamathematical extensibility in type theory," Ph.D Thesis, Cornell University (1987).
- [20] Sh. Noguchi, Y. Kojima, and J. Halbritter, "Measurement of a superconducting 500 MHz Nb cavity in the TM010-Mode," *Nucl. Instr. Meth.* vol. 179, p. 205, 1981.
- [21] Y. M. Li et al., "Research on field emission and dark current in ILC cavities," in *Proc. SRF2013*, Paris, France, Sept. 2013, pp. 392-397.
- [22] Q. S. Shu et al., "Experience in design, construction and application of a rotating T-R mapping system in superfluid He for TESLA 9-cell cavities," in *Proc. SRF1995*, Gif-sur-Yvette, France 1995, pp. 523-527.
- [23] S. Musser et al., "X-Ray imaging of superconducting RF cavities," in *Proc. SRF2005*, Ithaca, NY, USA, July 2005, pp. 295-299.
- [24] I. Ben-Zvi, J. F. Crawford, J. P. Turneure, "Electron multiplication in cavities," *IEEE Trans. Nucl. Sci.*, vol. NS-20, p. 54, 1973.
- [25] T. Grimm et al., "Superconducting RF activities at NSCL," in *Proc. SRF2001*, Tsukuba, Japan, Sept. 2001, pp. 86-90.
- [26] W. Bayer et al., *Nucl. Instr. Meth. A* 575(2007)321.
- [27] P. L. Anthony et al., *Nucl. Instr. Meth. A* 612(2009)1.
- [28] R. L. Geng et al., "First attempt at cavity x-ray detection in a CEBAF cryomodule for field emission monitoring," in *Proc. IPAC'15*. WEPWI012, pp. 3515-3517 (2015).
- [29] A. Freyberger, "Commissioning and operation of 12 GeV CEBAF," MOXGB2, *Proc. IPAC'15* pp. 1-5 (2015).
- [30] C. B. Duke and M. E. Alferieff, "Field Emission through Atoms Adsorbed on a Metal Surface," *J. Chem. Phys.*, vol. 46, p. 923, 1967.
- [31] J. W. Gadzuk and E.W. Plummer, "Field Emission Energy Distribution (FEED)," *Rev. Mod. Phys.*, vol. 45, p. 487, 1973.
- [32] R. Legg, Jefferson Lab internal report, JLAB-TN-16-034 (2016).
- [33] R. L. Geng, Jefferson Lab internal report, JLAB-TN-17-030 (2017).
- [34] J. Perry et al., "The CEBAF beam loss sensors," *Proc. PAC1993*, Pp 2184-2186 (1993).
- [35] J. Benesch, arXiv:physics/0606141, "Field Emission in CEBAF's Superconducting RF cavities and implications for future accelerators" <https://arxiv.org/abs/physics/0606141>

- [36] J. Benesch, arXiv:1502.06877 "A longitudinal study of field emission in CEBAF's SRF cavities 1995-2015"  
<https://arxiv.org/abs/1502.06877>
- [37] R. L. Geng, Jefferson Lab internal report, JLAB-TN-17-027 (2017).